Theoretical Study of Hydrogen Bonds Between Acetylene and Selected Proton Donor Systems

A. BENDE,[1,4] Á. VIBÓK,[2] G. J. HALÁSZ,[3] S. SUHAI[4]

[1]*National Institute for Research and Development of Isotopic and Molecular Technologies, Donath Street 71-103, P.O. Box 700, RO-3400, Cluj-Napoca, Romania*

[2]*Department of Theoretical Physics, Debrecen University, H-4010 Debrecen, P.O. Box 5, Hungary*

[3]*University of Debrecen Institute of Informatics, H-4010 Debrecen, P.O. Box 12, Hungary*

[4]*Molecular Biophysics Department, German Cancer Research Center, Im Neuenheimer Feld 280, D-69120, Heidelberg, Germany*

Received 12 February 2004; accepted 22 April 2004
Published online 10 September 2004 in Wiley InterScience (www.interscience.wiley.com).
DOI 10.1002/qua.20216

ABSTRACT: The equilibrium structures, the binding energies, and the second-order energy components of a series of hydrogen-bonded complexes involving acetylene are studied. The strength of the binding energy of the selected systems (HF . . . HCCH, HCl . . . HCCH, HCN . . . HCCH, and HCCH . . . HCCH) was different, ranging from a very weak interaction to a strong interaction. Calculations have been carried out at both the Hartree–Fock and correlated (second-order Møller–Plesset perturbation theory) levels of theory, using several different basis sets [6-31G(d,p), 6-311G(d,p), 6-31G++(d,p), 6-311G++(d,p), 6-31++G(2d,2p) and 6-311++G(2d,2p)]. The widely used a posteriori Boys–Bernardi counterpoise (CP) correction scheme has been compared with the a priori CHA/CE, CHA–MP2, and CHA–PT2 methods, using the chemical Hamiltonian approach (CHA). The results show that at both levels the CP and the appropriate CHA results are very close to each other. Only the monomer-based CHA-PT2 theory gives slightly overcorrected results, reflecting that the charge transfer and polarization effects are not taken into account in this method up to second order. We have also applied our earlier developed energy decomposition scheme in order to decompose the second-order energy contribution into different physically meaningful components. The results show that at large and intermediate intermolecular distances,

Correspondence to: Á. Vibók; e-mail: vibok@cseles.atomki.hu
Contract grant sponsor: OTKA.
Contract grant number: T037994.
Contract grant sponsor: Hungarian Academy of Sciences.
Contract grant sponsor: European Union.
Contract grant number: BMH4-CT96-1618.

the second-order intermolecular contribution is almost equal to the sum of different physically meaningful components (e.g., polarization, charge transfer, dispersion), while at shorter distances the slightly strong overlap effects fairly disturb this simple additivity. Int J Quantum Chem 101: 186–200, 2005

Key words: basis set superposition error; chemical Hamiltonian approach; intermolecular interactions; intermolecular perturbation theory

1. Introduction

It is well known that hydrogen bonds play a key role in biochemistry and biophysics, so their accurate treatment is essential. At the theoretical level, several quantum mechanical studies have been performed in order to study these interactions between different systems [1–4]. Most of the calculations are based on the supermolecular approach, in which the interaction energy of the studied dimer is obtained as an energy difference between the supermolecule and the monomers. However, this interaction energy often shows minima that are too deep, especially for the case of weak hydrogen bonds as the consequence of using finite basis sets in the calculations. This phenomenon is called basis set superposition error (BSSE) and it is attributable to the fact that the description of the monomer is actually better within the supermolecule than that for the free monomers by applying the same basis set. Thus, the BSSE is a purely mathematical effect that appears only as a result of the use of finite basis sets, leading to an incomplete description in the individual monomers. Several numerical studies and analytical considerations [5–7] show that the amount of this BSSE effect can be very large even for fairly large basis sets, so removing it in the practical calculations is very important.

In our earlier works [8–11], we demonstrated that these errors affect not only the interaction energies, but also their first- and second-order derivatives, which can produce different changes in geometry structures and harmonic vibrational frequency values. This effect was also shown by other investigators [12, 13] in the case of NCH . . . O_3, HCCH . . . O_3, and $(HF)_n$, $n = 3, 4$ systems.

One of our purposes in the present work is to calculate the structure of the interaction energy minima and second-order energy components (charge-transfer, polarization, dispersion, mixed charge-transfer polarization, and cross-components) for selected hydrogen-bonded (C—H . . . π) systems at the level of both Hartree–Fock (HF) and second-order Møller–Plesset perturbation theory (MP2), properly taking into account the BSSE. To treat this latter effect, we use both the well-known a posteriori counterpoise correction (CP) scheme developed by Jansen and Ross [14] and, independently, by Boys and Bernardi [15], as well as the a priori-type chemical Hamiltonian approach (CHA) constructed by Mayer [16, 17]. While in the former approach the monomers are adjusted to the dimer problem and the energies and other quantities of the free monomers become distance dependent, the CHA permits us to identify those terms of the Hamiltonian that are responsible for the BSSE effects. By omitting these terms, one can obtain wave functions free from artificial nonphysical delocalizations. Using this CHA scheme, several different approaches have been developed at both the HF [18–29] and correlated [30–38] levels of theory.

In contrast, we have also performed second-order energy component analysis using a decomposition scheme that was earlier developed based on the CHA framework [39]. We study how depend the different energy components in the second-order interaction energy correction from the strength of the hydrogen bonds and also from the basis sets are applied.

The next section provides a brief description of the methods employed. Next, the results for the Acetylene (Ac) dimer, Ac . . . HCN, Ac . . . HCl, and Ac . . . HF molecular systems are presented in several different basis sets and the interaction energies and their components are compared and discussed. The conclusions are presented in the final section.

2. Computational Methods

This section presents a brief summary of the applied CHA methods (CHA/CE, CHA–MP2, and CHA–PT2) and the CHA–PT2 energy decomposition procedure presented in earlier papers [14–16].

2.1. CHA/CE SCHEME

A conceptually different way of handling the BSSE problem is to apply the a priori CHA developed by Mayer [16, 17]. The CHA procedure permits the supermolecule calculations to remain consistent with those for the free monomer performed in their original basis sets. The most important aspect of Mayer's approach is that one can divide the Hamiltonian into two parts and omit those terms that are responsible for the BSSE:

$$\hat{H}_{\mathrm{BO}} = \hat{H}_{\mathrm{CHA}} + \hat{H}_{\mathrm{BSSE}}, \tag{1}$$

where $\hat{H}_{\mathrm{BO}}$ is the original Born–Oppenheimer Hamiltonian, $\hat{H}_{\mathrm{CHA}}$ is the BSSE-free part of the Hamiltonian, while the second term on the right-hand side corresponds to the BSSE. It should be emphasized that because BSSE is not a physical quantity, one cannot expect that the remaining part of the Hamiltonian $\hat{H}_{\mathrm{CHA}}$ to be Hermitian. Applying this non-Hermitian BSSE-free CHA Hamiltonian $\hat{H}_{\mathrm{CHA}}$ and using the method of momenta instead of the variational principle appropriate Hartree–Fock-type CHA–SCF [19], equations were derived in order to calculate BSSE-free wave functions:

$$\hat{H}_{\mathrm{CHA}}\Psi_{\mathrm{CHA}} = \Lambda\Psi_{\mathrm{CHA}}. \tag{2}$$

As a result of several numerical and analytical considerations [24–27] using this BSSE-free wave function, the energy of the system can be calculated as a conventional expectation value of the original Born–Oppenheimer Hamiltonian and not of the chemical one. This is indicated by the expression, CHA with conventional energy (CHA/CE). Here is our working formula:

$$E_{\mathrm{CHA/CE}} = \frac{\langle\Psi_{\mathrm{CHA}}|\hat{H}_{\mathrm{BO}}|\Psi_{\mathrm{CHA}}\rangle}{\langle\Psi_{\mathrm{CHA}}|\Psi_{\mathrm{CHA}}\rangle}. \tag{3}$$

2.2. SUPERMOLECULE CHA–MP2 THEORY

While to obtain Hartree–Fock-type equations from the CHA Hamiltonian is a relatively straightforward procedure, the generalization of it to the Møller–Plesset perturbation theory was a bigger task. As it was shown by Mayer [38], the appropriate second-order energy can be obtained as follows. First, one has to calculate the first-order CHA wave function χ using the non-Hermitian CHA Hamiltonian partitioned as $\hat{H}_{\mathrm{CHA}} = \hat{H}^0 + \hat{V}_{\mathrm{CHA}}$, where $\hat{H}^0$ is the unperturbed Hamiltonian. This latter one is built up from the CHA canonic molecular orbitals and orbital energies, which are the solutions of the appropriate CHA–SCF equations. It can be seen that the perturbed $\hat{V}_{\mathrm{CHA}}$ operator is also non-Hermitian. The original Hermitian Born–Oppenheimer Hamiltonian $\hat{H}_{\mathrm{BO}}$ can also be partitioned as a sum of the same non-Hermitian unperturbed Hamiltonian $\hat{H}^0$ and some new (also non-Hermitian) perturbation $\hat{V}$: $\hat{V} = \hat{H}_{\mathrm{BO}} - \hat{H}^0$. Using the first-order CHA wave function χ, the generalized Hylleraas functional J_2 can easily be calculated:

$$J_2 = \frac{1}{\langle\Psi_0|\Psi_0\rangle}\,[2\ \mathrm{Re}(\langle\hat{Q}\chi|\hat{V}|\Psi_0\rangle) + \mathrm{Re}(\langle\chi|\hat{H}^0 - E_0|\chi\rangle)], \tag{4}$$

and the second-order energy will be given by

$$E^{(2)} = \frac{\langle\Psi_0|\hat{H}_{\mathrm{BO}}|\Psi_0\rangle}{\langle\Psi_0|\Psi_0\rangle} + J_2, \tag{5}$$

where Ψ_0 is the unperturbed wave function, E_0 is the zero-order energy ($\hat{H}^0\Psi_0 = E_0\Psi_0$), and $\hat{Q}$ is the projection operator to the orthogonal complement to Ψ_0. These equations define our working formula at the second-order perturbation level. This formalism is called CHA–MP2 theory [32].

2.3. MONOMER-BASED CHA–PT2 THEORY

In this perturbation theory, only the orbitals and orbital energies on which $\hat{H}^0$ is built up differ from the previous case. Namely, here one starts from the orbitals and orbital energies of the unperturbed free monomers. The zero-order effective one-electron Hamiltonian can be defined as the sum of the "effective" monomer Hartree–Fock operators. The unperturbed ground-state wave functions are chosen as the antisymmetrized product of the monomer ground-state wave functions. Applying the following perturbation $\hat{V}_{\mathrm{CHA}}$: ($\hat{V}_{\mathrm{CHA}} = \hat{H}_{\mathrm{CHA}} - \hat{H}^0$), the first-order wave function can also be obtained and the second-order BSSE-free energy contribution can be calculated from Eq. (5) as before.

2.4. CHA–PT2 ENERGY DECOMPOSITION

In order to perform the decomposition of the second-order energy contribution in the CHA–PT2

framework, we should go back to the appropriate first-order CHA wave function χ, which is

$$|\chi\rangle = \tfrac{1}{4}\sum_{i,j\in A}^{\text{occ}}\sum_{p,q\in A}^{\text{virt}}\frac{-[pq\|ij]}{\varepsilon_p+\varepsilon_q-\varepsilon_i-\varepsilon_j}|\Psi_{ij}^{pq}\rangle + \sum_{i\in A}^{\text{occ}}\sum_{p}^{\text{virt}}\frac{-\langle\tilde{p}|\hat{V}_B^{\text{aux}}|i\rangle}{\varepsilon_p-\varepsilon_i}|\Psi_i^p\rangle + \tfrac{1}{4}\sum_{i\in A}^{\text{occ}}\sum_{j\in B}^{\text{occ}}\sum_{p,q}^{\text{virt}}\frac{-[\tilde{p}\tilde{q}\|ij]}{\varepsilon_p+\varepsilon_q-\varepsilon_i-\varepsilon_j}\|\Psi_{ij}^{pq}\rangle + (A\leftrightarrow B), \quad (6)$$

where $(A \leftrightarrow B)$ indicates that all terms with monomers A and B interchanged should be added. $|\Psi_i^p\rangle$ and $|\Psi_{ij}^{pq}\rangle$ are singly and doubly excited determinants in terms of the occupied and virtual monomer orbitals. V_B^{aux} is an auxiliary operator, defined through its matrix element as

$$\langle\tilde{p}|\hat{V}_B^{\text{aux}}|i\rangle = \left\langle\tilde{p}\left|\sum_{a\in B}\frac{-Z_a}{r_a}\right|i\right\rangle + \sum_{j\in B}^{\text{occ}}\lceil\ \tilde{p}\tilde{j}\|ij\ \rceil. \quad (7)$$

It can be seen that the first-order wave function Eq. (6) is nothing other than the sum of different terms that have well-defined physical meaning:

$$|\chi\rangle = |\chi\rangle_{\text{intra-corr}} + |\chi\rangle_{\text{pol}} + |\chi\rangle_{\text{CT}} + |\chi\rangle_{\text{disp}} + |\chi\rangle_{\text{pol-CT}}. \quad (8)$$

In this sum, the first term $|\chi\rangle_{\text{intra-corr}}$ gives the intramolecular correlation of the free monomers:

$$|\chi\rangle_{\text{intra-corr}} = \tfrac{1}{4}\sum_{i,j\in A}^{\text{occ}}\sum_{p,q\in A}^{\text{virt}}\frac{-[pq\|ij]}{\varepsilon_p+\varepsilon_q-\varepsilon_i-\varepsilon_j}|\Psi_{ij}^{pq}\rangle + (A\leftrightarrow B). \quad (9)$$

The $|\chi\rangle_{\text{pol}}$ comes from the second term of Eq. (5), when the occupied and virtual orbitals are on the same monomer. This term is called polarization:

$$|\chi\rangle_{\text{pol}} = \sum_{i\in A}^{\text{occ}}\sum_{p\in A}^{\text{virt}}\frac{-\langle\tilde{p}|\hat{V}_B^{\text{aux}}|i\rangle}{\varepsilon_p-\varepsilon_i}|\Psi_i^p\rangle + (A\leftrightarrow B). \quad (10)$$

If the occupied and virtual orbitals are on different monomers under the summations, the former expression will describe the CT-type effects between the monomers:

$$|\chi\rangle_{\text{CT}} = \sum_{i\in A}^{\text{occ}}\sum_{p\in B}^{\text{virt}}\frac{-\langle\tilde{p}|\hat{V}_B^{\text{aux}}|i\rangle}{\varepsilon_p-\varepsilon_i}|\Psi_i^p\rangle + (A\leftrightarrow B). \quad (11)$$

The third term in Eq. (5) gives the conventional dispersion-type excitations if the virtual orbitals are on different monomers:

$$|\chi\rangle_{\text{disp}} = \tfrac{1}{2}\sum_{i\in A}^{\text{occ}}\sum_{j\in B}^{\text{occ}}\sum_{p\in A}^{\text{virt}}\sum_{q\in B}^{\text{virt}}\frac{-[\tilde{p}\tilde{q}\|ij]}{\varepsilon_p+\varepsilon_q-\varepsilon_i-\varepsilon_j}|\Psi_{ij}^{pq}\rangle + (A\leftrightarrow B). \quad (12)$$

If the virtual orbitals are on the same monomers, one can obtain a mixed term that corresponds to the combined polarization–CT component of the first-order wave function:

$$|\chi\rangle_{\text{pol-CT}} = \tfrac{1}{2}\sum_{i\in A}^{\text{occ}}\sum_{j\in B}^{\text{occ}}\sum_{p,q\in A}^{\text{virt}}\frac{-[\tilde{p}\tilde{q}\|ij]}{\varepsilon_p+\varepsilon_q-\varepsilon_i-\varepsilon_j}|\Psi_{ij}^{pq}\rangle + (A\leftrightarrow B). \quad (13)$$

Using the above-described decomposition of the first-order wave function, one can explicitly place the different components of the first-order wave function into Eq. (4), in order to obtain the explicit formulae for the different BSSE-free second-order interaction energy contributions that have special physical meaning: J_2^{pol}, J_2^{CT}, J_2^{disp}, and $J_2^{\text{pol–CT}}$. It can also be introduced the remaining term (denoted cross-term) describing all overlap-caused interferences as the difference of the total J_2 and of the physical terms:

$$J_2^{\text{cross-term}} = J_2 - [J_2^{\text{pol}} + J_2^{\text{CT}} + J_2^{\text{disp}} + J_2^{\text{pol–CT}} + E_A^{(2)} + E_B^{(2)}]. \quad (14)$$

Explicit expressions for the different J_2 components are given in Ref. [39]. We refer to this article for further details.

3. Computational Details

The calculations were carried out partly in Heidelberg on a Hewlett-Packard cluster and partly in Debrecen on a Pentium 200 PC and Compaq Alpha

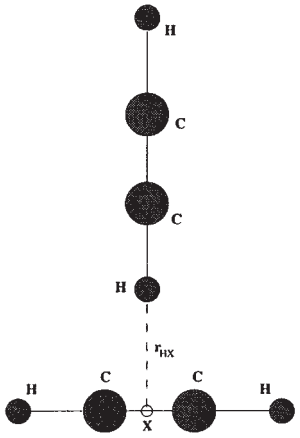

FIGURE 1. Acetylene–acetylene geometry.

running under Linux. The standard HF, MP2, and CP-corrected HF, MP2 calculations were performed by the Gaussian 98 computer code [40]. The CHA/CE, CHA–MP2, CHA–PT2, and CHA–PT2-ED (energy decomposition)-type calculations were carried out by generating the input data (integrals and RHF orbitals) with a slightly modified version of HONDO-8 [41].

In these calculations, the CHA–SCF code [19], the CHA–MP2 program of Mayer and Valiron [32, 34], the CHA–PT2 [30, 31], and the CHA–PT2-ED [39] were used. The different acetylene–complex geometries were optimized using conventional Hartree–Fock and second-order Møller–Plesset perturbation theories for each basis set. We considered different standard Pople basis sets: 6-31G, 6-311G, 6-31++G, 6-311++G, 6-31G(d,p), 6-311G(d,p), 6-31++G(d,p), 6-311++G(d,p), 6-31++G(2d,2p), and 6-311++G(2d,2p).

The conventional supermolecule geometries were optimized at both the HF and MP2 levels,

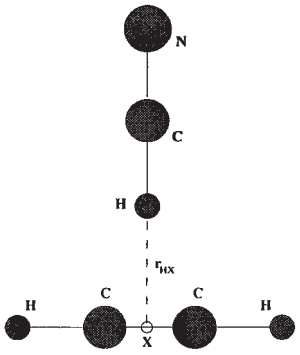

FIGURE 2. Acetylene–HCN geometry.

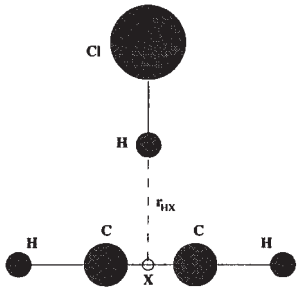

FIGURE 3. Acetylene–HCl geometry.

applying the analytical gradient method included in the Gaussian 98, while the CHA and CP-corrected geometries were calculated by using numerical gradient method (inverse parabolic interpolation [42]) in internal coordinates, considering only the intermolecular coordinates (one bond, two angles, and three torsion angles) as geometry variables. To test the applicability of our numerical gradient method, we have performed several sample calculations using both this latter method and the analytical gradient technique built into the Gaussian 98 program. As a consequence, there is practically no difference between them for conventional uncorrected cases.

4. Results and Discussion

The calculated results are summarized in four tables from the weakest systems up to the stronger interacting ones. Table I shows the values obtained for the geometry (r_{HX}) and the binding energy (ε_{Ac-Ac}) of the Ac . . . Ac dimer, using the conventional, CHA and BB schemes at both the Hartree–Fock and second-order (MP2 and PT2-type) perturbation levels of theory. In Table II, Table III, and Table IV, similar results are given for the Ac . . . HCN, Ac . . . HCl, and Ac . . . HF dimers, re-

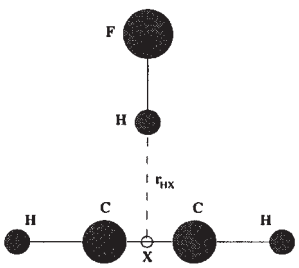

FIGURE 4. Acetylene–HF geometry.

TABLE I

r_{HX} intermolecular distance (in Å) and the ε_{Ac-Ac} intermolecular binding energy (in mH) for acetylene–acetylene complex computed with Hartree–Fock (SCF, CHA–SCF, CP–SCF) and second-order many-body perturbation theories (MP2, CHA–MP2, CHA–PT2, CP–MP2), using 6-31G(d,p), 6-311G(d,p), 6-31++G(d,p), 6-311++G(d,p), 6-31++G(2d,2p), and 6-311++G(2d,2p) basis sets. The number of basis functions is given in parentheses.

Basis set	Method	r_{HX}	ε_{Ac-Ac}	Method	r_{HX}	ε_{Ac-Ac}
6-31G(d,p)	SCF	2.94820	−2.062	MP2	2.63614	−3.340
(80)	CP–SCF	2.99233	−1.334	CP–MP2	2.81460	−1.831
	CHA–SCF	2.96849	−1.555	CHA–MP2	2.76321	−2.096
		—	—	CHA–PT2	2.75428	−2.306
6-311G(d,p)	SCF	3.03381	−1.527	MP2	2.74232	−2.639
(100)	CP–SCF	3.07364	−1.202	CP–MP2	2.85032	−1.786
	CHA–SCF	3.03954	−1.308	CHA–MP2	2.83744	−1.876
		—	—	CHA–PT2	2.80003	−2.236
6-31++G(d,p)	SCF	3.05348	−1.281	MP2	2.63438	−3.254
(100)	CP–SCF	3.08834	−1.122	CP–MP2	2.85429	−1.662
	CHA–SCF	3.08194	−1.125	CHA–MP2	2.85087	−1.707
		—	—	CHA–PT2	2.84801	−1.994
6-311++G(d,p)	SCF	3.07575	−1.265	MP2	2.69877	−3.136
(120)	CP–SCF	3.10959	−1.104	CP–MP2	2.84345	−1.770
	CHA–SCF	3.10526	−1.120	CHA–MP2	2.83835	−1.772
		—	—	CHA–PT2	2.83193	−2.110
6-31++G(2d,2p)	SCF	3.04418	−1.302	MP2	2.68119	−2.988
(136)	CP–SCF	3.06961	−1.182	CP–MP2	2.77396	−1.998
	CHA–SCF	3.07314	−1.139	CHA–MP2	2.77858	−2.126
		—	—	CHA–PT2	—	—
6-311++G(2d,2p)	SCF	3.07063	−1.347	MP2	2.69619	−2.621
(156)	CP–SCF	3.08962	−1.041	CP–MP2	2.74883	−2.127
	CHA–SCF	3.08458	−1.133	CHA–MP2	2.74192	−2.112
		—	—	CHA–PT2	—	—

spectively. Figures 1–4 present the equilibrium geometries for the four studied systems. Figures 5–12 show the different components of the perturbation expansion (E_{H-L}, Heitler–London energy; J_2, second-order energy correction; J_2^{phys}, second-order "physical" term; J_2^{cross}, second-order cross term; and E_2, total second-order energy), as well as the five different components of the J_2 energy (J_2^{pol}, polarization; J_2^{CT}, charge-transfer; J_2^{disp}, dispersion; J_2^{pol-CT}, combined polarization and charge-transfer; and J_2^{cross}, second-order cross term) for all four dimers.

BSSE-FREE GEOMETRIES AND INTERACTION ENERGIES

Scheiner and Grabowski [1] presented an accurate theoretical study for the molecular interaction of the acetylene with different small proton acceptor complexes. These investigators studied the equilibrium geometries, the interaction energies, and the different proton donor molecular and intermolecular deformations. In their work, they calculated the BSSE corrections only in the interaction energies. In the present study, our aim is to study the BSSE effects not only in the interaction energies, but in the geometry conformations as well.

Ac . . . Ac

The weakest interacting system in our investigation is the Acetylene–Acetylene dimer for which the configuration is presented in Figure 1. The equilibrium geometry and the binding energy for this system were calculated for the uncorrected, the CP and CHA-corrected cases at both the Hartree–Fock

TABLE II

r_{HX} intermolecular distance (in Å) and the ε_{Ac-HCN} intermolecular binding energy (in mH) for acetylene–HCN complex computed with Hartree–Fock (SCF, CHA–SCF, CP–SCF) and second-order many-body perturbation theories (MP2, CHA–MP2, CHA–PT2, CP–MP2), using 6-31G(d,p), 6-311G(d,p), 6-31++G(d,p), 6-311++G(d,p), 6-31++G(2d,2p), and 6-311++G(2d,2p) basis sets. The number of basis functions is given in parentheses.

Basis set	Method	r_{HX}	ε_{Ac-HCN}	Method	r_{HX}	ε_{Ac-HCN}
6-31G(d,p)	SCF	2.72682	−3.568	MP2	2.52007	−4.999
(75)	CP–SCF	2.75640	−3.029	CP–MP2	2.64855	−3.331
	CHA–SCF	2.74136	−3.353	CHA–MP2	2.62165	−3.683
				CHA–PT2	2.59951	−4.016
6-311G(d,p)	SCF	2.81812	−3.004	MP2	2.61262	−3.982
(94)	CP–SCF	2.84409	−2.633	CP–MP2	2.69865	−3.041
	CHA–SCF	2.83091	−2.766	CHA–MP2	2.69300	−3.139
				CHA–PT2	2.65029	−3.855
6-31++G(d,p)	SCF	2.81133	−2.739	MP2	2.53255	−4.657
(94)	CP–SCF	2.83107	−2.539	CP–MP2	2.69177	−2.932
	CHA–SCF	2.82736	−2.512	CHA–MP2	2.68835	−3.023
				CHA–PT2	2.68857	−3.496
6-311++G(d,p)	SCF	2.84459	−2.631	MP2	2.59507	−4.343
(113)	CP–SCF	2.86560	−2.422	CP–MP2	2.69466	−2.975
	CHA–SCF	2.86320	−2.464	CHA–MP2	2.67959	−3.037
			—	CHA–PT2	—	—
6-31++G(2d,2p)	SCF	2.80059	−2.795	MP2	2.55980	−4.319
(127)	CP–SCF	2.81406	−2.620	CP–MP2	2.61916	−3.361
	CHA–SCF	2.81245	−2.563	CHA–MP2	2.62203	−3.508
				CHA–PT2	2.62404	−4.048
6-311++G(2d,2p)	SCF	2.82597	−2.731	MP2	2.55379	−4.049
(146)	CP–SCF	2.83359	−2.615	CP–MP2	2.60199	−3.482
	CHA–SCF	2.83361	−2.553	CHA–MP2	2.59865	−3.441
				CHA–PT2	—	—

and second-order Møller–Plesset perturbation levels of theory, using six different basis sets. [Calculations with the CHA–PT2 method using 6-31++G(2d,2p) and 6-311++G(2d,2p) basis sets are missing because of the large memory usage.] In Table I we can observe the BSSE dependence of the r_{HX} distance, especially for smaller basis sets, but this effect decreases as the basis set applied becoming more complete. In case of the 6-311++G(2d,2p) basis set we found ≈0.02 Å and ≈0.05 Å differences between the uncorrected and the BSSE-corrected results for HF and MP2 levels. In contrast, it can be emphasized that these corrections are not so significant at the HF level, but at the perturbation level they are still important. Similar statement can be drawn for the binding energies presented in the same table. In this case, the magnitude of the BSSE corrections are more considerable, they are about 8–15% from the value of the interaction energies. Moreover, the second-order component in the binding energy is almost double, about $\Delta E^{(2)} - \Delta E^{HF} \approx -1.0$ mH compared with the HF results, which allow us to carry out far more accurate calculations with the MP4 perturbation method. From this latter calculation (which we have performed), we found that the difference between the CP-corrected second-order and the fourth-order corrections, using the 6-31++G(2d,2p) basis set is not so important ($\Delta E^{(4)} - \Delta E^{(2)} \approx 0.18$ mH).

Ac . . . HCN

The second molecular complex that was selected to our investigation is the Acetylene–HCN system, which forms a slightly stronger complex than the Acetylene–Acetylene dimer. Similar methods and

TABLE III

r_{HX} intermolecular distance (in Å) and the ε_{Ac-HCl} intermolecular binding energy (in mH) for acetylene–HCl complex computed with Hartree–Fock (SCF, CHA–SCF, CP–SCF) and second-order many-body perturbation theories (MP2, CHA–MP2, CHA–PT2, CP–MP2), using 6-31G(d,p), 6-311G(d,p), 6-31++G(d,p), 6-311++G(d,p), 6-31++G(2d,2p), and 6-311++G(2d,2p) basis sets. The number of basis functions is given in parentheses.

Basis set	Method	r_{HX}	ε_{Ac-HCl}	Method	r_{HX}	ε_{Ac-HCl}
6-31G(d,p)	SCF	2.58591	−3.719	MP2	2.38026	−5.375
(64)	CP–SCF	2.65698	−2.798	CP–MP2	2.52444	−3.562
	CHA–SCF	2.59997	−3.103	CHA–MP2	2.51570	−3.769
				CHA–PT2	2.51100	−3.939
6-311G(d,p)	SCF	2.70914	−2.864	MP2	2.44384	−4.331
(83)	CP–SCF	2.73921	−2.532	CP–MP2	2.53906	−3.428
	CHA–SCF	2.72487	−2.644	CHA–MP2	2.51309	−3.573
				CHA–PT2	2.55655	−3.751
6-31++G(d,p)	SCF	2.69147	−2.655	MP2	2.40457	−5.162
(79)	CP–SCF	2.74092	−2.285	CP–MP2	2.57115	−3.088
	CHA–SCF	2.73520	−2.268	CHA–MP2	2.57994	−3.069
				CHA–PT2	2.58954	−3.315
6-311++G(d,p)	SCF	2.72949	−2.540	MP2	2.43450	−4.969
(98)	CP–SCF	2.77807	−2.226	CP–MP2	2.55728	−3.184
	CHA–SCF	2.77595	−2.253	CHA–MP2	2.53799	−3.267
				CHA–PT2	2.61669	−3.372
6-31++G(2d,2p)	SCF	2.69983	−2.523	MP2	2.34086	−5.265
(106)	CP–SCF	2.72977	−2.323	CP–MP2	2.41242	−4.064
	CHA–SCF	2.73114	−2.250	CHA–MP2	2.44315	−3.970
				CHA–PT2	2.51325	−3.968
6-311++G(2d,2p)	SCF	2.73871	−2.445	MP2	2.33442	−5.130
(125)	CP–SCF	2.75334	−2.258	CP–MP2	2.40203	−4.210
	CHA–SCF	2.75454	−2.196	CHA–MP2	2.38542	−4.282
				CHA–PT2	2.48544	−4.169

basis sets to those in the previous case were used to find the optimized geometry structures and their interaction energies. The results are presented in Table II. Because of the similar memory requirement to that in the previous case, we were unable to perform our calculation with the CHA–PT2 method using the 6-311++G(2d,2p) basis set. As for the 6-311++G(d,p) basis, it was fairly complicated to perform the optimization procedure because the potential energy surface (PET) is almost flat. In this case, the BSSE corrections at the HF level for the r_{HX} distance are not so important (≈0.015 Å), while at the second-order perturbation level they are still reasonably large quantities (≈0.05 Å). A similar tendency holds for the binding energies, where we obtained ≈−0.1 mH for the HF methods and 0.6–1.0 mH for the correlated level. Even using the largest 6-311++G(2d,2p) basis set, the difference between the MP2 and the MP4 results is: $\Delta E^{(4)} - \Delta E^{(2)} \approx 0.2$ mH, which is almost five times smaller than this one between the appropriate HF and MP2 calculations ($\Delta E^{(2)} - \Delta E^{HF} \approx -0.9$ mH). The experimental values [43, 44] obtained for the $r_{CX} = 3.655$ Å are in good agreement with our BSSE-free results: 3.666 Å for the MP2–CHA/6-311++G(2d,2p) and 3.669 Å for the MP2–CP/6-311++G(2d,2p).

Ac . . . HCl

Table III presents the results for the Acetylene–HCl dimer. The optimized geometry and the binding energy were calculated similarly to the first and second cases. For this system, we were able to obtain converged results for all the applied basis sets. It was found that even including polarization and diffuse functions in the basis

TABLE IV

r_{HX} intermolecular distance (in Å) and the ε_{Ac-HF} intermolecular binding energy (in mH) for acetylene–HF complex computed with Hartree–Fock (SCF, CHA–SCF, CP–SCF) and second-order many body perturbation theories (MP2, CHA–MP2, CHA–PT2, CP–MP2), using 6-31G(d,p), 6-311G(d,p), 6-31++G(d,p), 6-311++G(d,p), 6-31++G(2d,2p), and 6-311++G(2d,2p) basis sets. The number of basis functions is given in parentheses.

Basis set	Method	r_{HX}	ε_{Ac-HF}	Method	r_{HX}	ε_{Ac-HF}
6-31G(d,p)	SCF	2.34731	−6.025	MP2	2.18251	−7.917
(60)	CP–SCF	2.40959	−4.921	CP–MP2	2.33711	−5.202
	CHA–SCF	2.38622	−5.189	CHA–MP2	2.32204	−5.458
				CHA–PT2	2.36319	−5.539
6-311G(d,p)	SCF	2.36702	−5.268	MP2	2.15495	−6.918
(75)	CP–SCF	2.45122	−4.309	CP–MP2	2.34799	−4.634
	CHA–SCF	2.44020	−4.475	CHA–MP2	2.31748	−4.982
				CHA–PT2	2.36236	−5.313
6-31++G(d,p)	SCF	2.38809	−4.813	MP2	2.16810	−7.350
(75)	CP–SCF	2.40277	−4.601	CP–MP2	2.27327	−5.445
	CHA–SCF	2.40398	−4.575	CHA–MP2	2.28340	−5.347
				CHA–PT2	2.38930	−5.171
6-311++G(d,p)	SCF	2.40966	−4.752	MP2	2.17910	−6.978
(90)	CP–SCF	2.41619	−4.358	CP–MP2	2.26696	−5.158
	CHA–SCF	2.41379	−4.392	CHA–MP2	2.24481	−5.318
				CHA–PT2	2.34807	−5.131
6-31++G(2d,2p)	SCF	2.34020	−4.915	MP2	2.10752	−7.565
(102)	CP–SCF	2.34950	−4.727	CP–MP2	2.17169	−6.303
	CHA–SCF	2.35354	−4.735	CHA–MP2	2.19966	−6.126
				CHA–PT2	2.29199	−5.930
6-311++G(2d,2p)	SCF	2.34811	−4.883	MP2	2.14221	−7.209
(117)	CP–SCF	2.36032	−4.741	CP–MP2	2.19561	−6.161
	CHA–SCF	2.36358	−4.669	CHA–MP2	2.18706	−6.205
				CHA–PT2	2.28946	−6.067

sets, the BSSE amounts for the r_{HX} distance at the HF level are almost negligible, while at the second-order perturbational level, these corrections are much larger (0.06–0.1 Å). For the binding energies, we obtained similar results; i.e., the HF-type corrections are insignificant, while the BSSE-corrected MP2 and PT2 results are more than 1.0 mH higher than the appropriate uncorrected MP2 values. Considering the MP4 calculation, a similar tendency holds to that in the case of our previously studied system, namely applying the largest basis set as 6-311++G(2d,2p) the difference in the interaction energies using the HF and MP2 methods is $\Delta E^{(2)} - \Delta E^{HF} \approx -1.9$ mH, while this quantity calculating the MP2 and MP4 corrections is $\Delta E^{(4)} - \Delta E^{(2)} \approx 0.6$ mH. It can also be commented that this latter one is the largest value among our studied systems. The experimental value is (r_{ClX} = 3.699 Å), given by Legon et al. [45], and the BSSE-corrected results give 3.665 Å for the MP2–CHA/6-311++G(2d,2p) and 3.682 Å for the MP2-CP/6-311++G(2d,2p).

Ac . . . HF

The strongest interacting system in this study is the Acetylene–HF dimer (see Table IV). The geometry optimization and the binding energy calculation were made using the same basis sets and methods as before. Accordingly, more or less the same conclusions can be drawn again for the r_{HX} intermolecular distance as in the earlier described cases. That is, the HF results do not show a reasonably large BSSE content, especially when the polarization and diffuse functions are included in the applied basis set. However, the MP2 corrections are

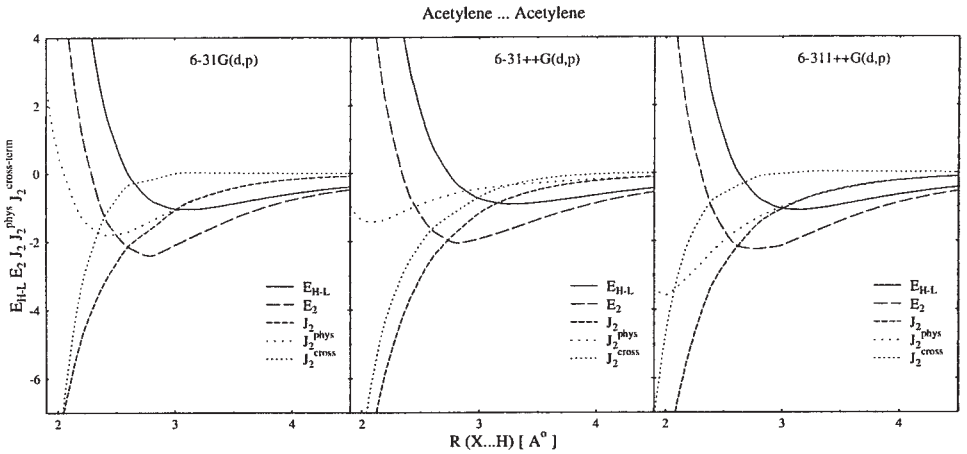

FIGURE 5. Potential curves of the Ac . . . Ac system calculated in three different basis sets [6-31G(d,p), 6-31++G(d,p), 6-311++G(d,p)] as a function of the r_{HX} hydrogen bond length. The curves display four different energy components: E_{H-L}, Heitler–London energy; J_2, second-order energy correction; J_2^{phys}, second-order "physical" term; J_2^{cross}, second-order "cross" term. E_2 is the total second-order energy.

still important. As for the binding energies, the HF level hardly gives any BSSE cerrection, but at the MP2 level, the energy differences remain ~1.5 mH. The difference between the MP2 and MP4 corrections in the 6-311++G(2d,2p) basis set is almost as great as in the first two cases where they were about $\Delta E^{(4)} - \Delta E^{(2)} \approx 0.11$ mH, while this quantity between the HF and MP2 corrections is much larger ($\Delta E^{(2)} - \Delta E^{HF} \approx -1.5$ mH). For this dimer, the experimental result is $r_{FX} = 3.075$ Å, obtained by Read and Flygàre [46], and the BSSE-free intermolecular distances are 3.113 Å for the MP2–CHA/6-311++G(2d,2p) and 3.122 Å for the MP2-CP/6-311++G(2d,2p).

4.2. SECOND-ORDER ENERGY

The calculations show that not only the second-order energy corrections itself, but also the BSSE content of these quantities in the interaction energies, are very important. To study these quantities systematically, we apply the CHA–PT2 second-order BSSE-free perturbation method. This scheme is able to handle the different components (charge-

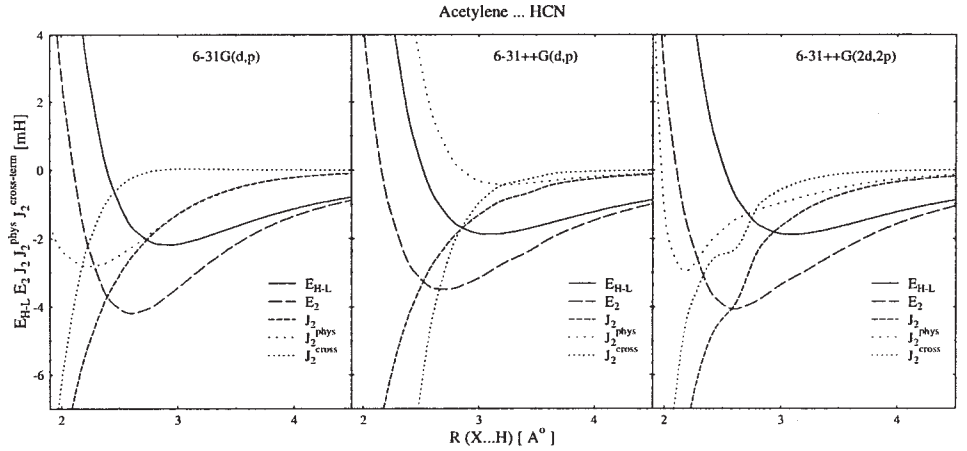

FIGURE 6. Potential curves of the Ac . . . HCN system calculated in three different basis sets [6-31G(d,p), 6-31++G(d,p), 6-31++G(2d,2p)] as a function of the r_{HX} hydrogen bond length. The curves display four different energy components: E_{H-L}, Heitler–London energy; J_2, second-order energy correction; J_2^{phys}, second-order "physical" term; J_2^{cross}, second-order "cross" term. E_2 is the total second-order energy.

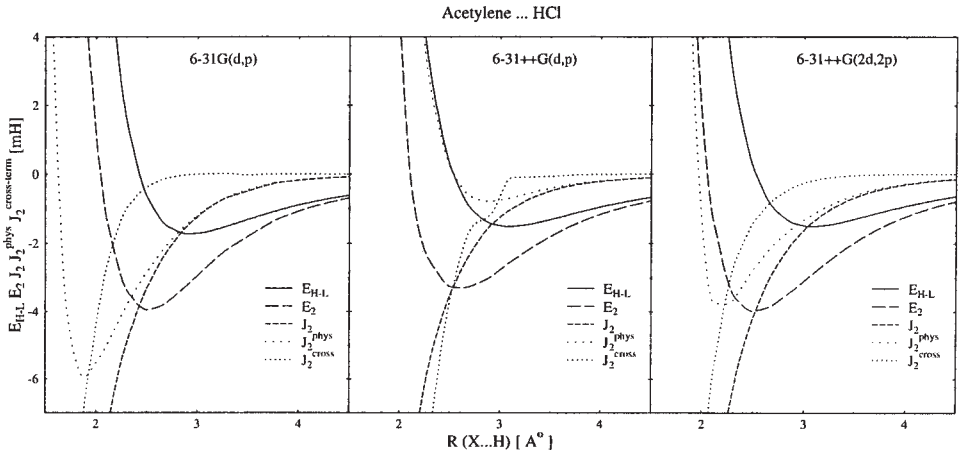

FIGURE 7. Potential curves of the Ac . . . HCl system calculated in three different basis sets [6-31G(d,p), 6-31++G(d,p), 6-31++G(2d,2p)] as a function of the r_{HX} hydrogen bond length. The curves display four different energy components: E_{H-L}, Heitler–London energy; J_2, second-order energy correction; J_2^{phys}, second-order "physical" term; J_2^{cross}, second-order "cross" term. E_2 is the total second-order energy.

transfer, polarization, dispersion, combined charge-transfer polarization, and cross-components) of the second-order energy, even if the SCF effects (polarization and delocalizations) are accounted for only up to second order. An overview of the results of our calculations is given in Figures 5–8: the total second-order energies (Fig. 5: Ac . . . Ac, Fig. 6: Ac . . . HCN, Fig. 7: Ac . . . HCl, and Fig. 8: Ac . . . HF) are compared with the Heitler–London ones representing the sum of the zero- and first-order PT contributions, the resulting second-order interaction contribution J_2, and its decomposition into "physical" and interference ("cross") components. It can be seen that the second-order results are strongly basis and system dependent, which is obvious because, for instance, the dispersion can be described appropriately only by using significantly large basis set. But at the same time, it can also be observed that the "cross"-component J_2^{cross} shows an important increase when we use diffuse functions together with d- and p-polarization ones, and that afterward, using 2d and 2p functions, the contribution of J_2^{cross} became smaller. At the short intermolecular distances, the contributions of the

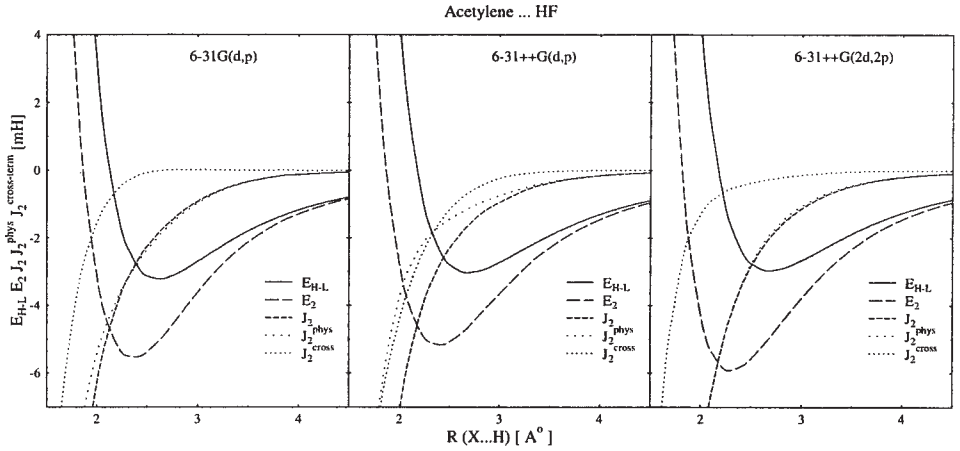

FIGURE 8. Potential curves of the Ac . . . HF system calculated in three different basis sets [6-31G(d,p), 6-31++G(d,p), 6-31++G(2d,2p)] as a function of the r_{HX} hydrogen bond length. The curves display four different energy components: E_{H-L}, Heitler–London energy; J_2, second-order energy correction; J_2^{phys}, second-order "physical" term; J_2^{cross}, second-order "cross" term. E_2 is the total second-order energy.

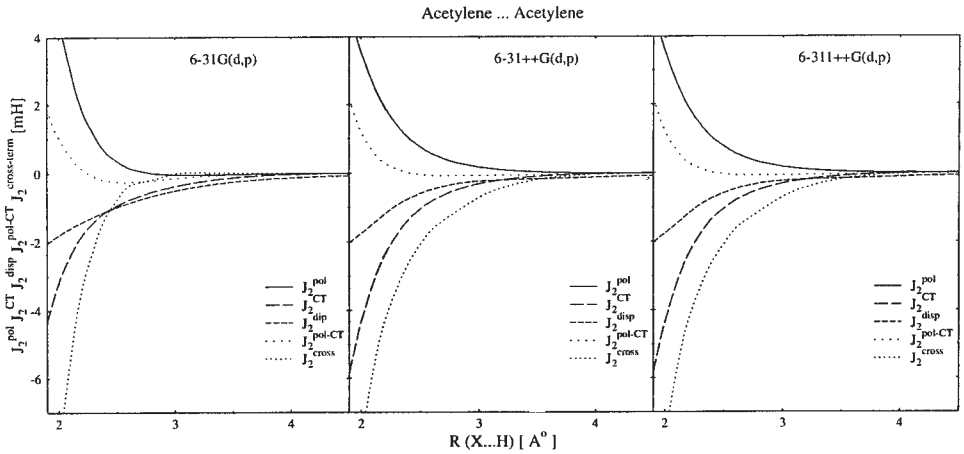

FIGURE 9. Energy components for the Ac . . . Ac system calculated in three different basis sets [6-31G(d,p), 6-31++G(d,p), 6-311++G(d,p)] as a function of the r_{HX} hydrogen bond length. The curves display five different components of the J_2 energy: J_2^{pol}, polarization; J_2^{CT}, charge-transfer; J_2^{disp}, dispersion; J_2^{pol-CT}, combined polarization and charge-transfer; J_2^{cross}, second-order "cross" term.

"physical" and "cross"-terms are quite different, while at very large intermolecular separations when the overlap tends to zero, the "cross-terms" would vanish. It can be observed that using (2d,2p) polarization functions, near the intermolecular minimum, the J_2^{cross} contribution is no longer dominant.

The individual second-order energy components (J_2^{pol}, polarization; J_2^{CT}, charge-transfer; J_2^{disp}, dispersion; J_2^{pol-CT}, combined polarization and charge-transfer, and J_2^{cross}, second-order "cross" term) discussed in section 2.4 are displayed in Figures 9–12. At large intermolecular separations the sum of the "physical" energy components is not distinguishable from the true second-order energy contribution, in accord with the expectation. For basis sets that do not contain diffuse functions, or that have more polarization functions, the "cross"-component remains comparatively small, even at shorter distances. When we use diffuse functions for which the intermolecular overlap becomes considerable, the behavior of the different energy components is not unambiguous. Following the magnitudes of the

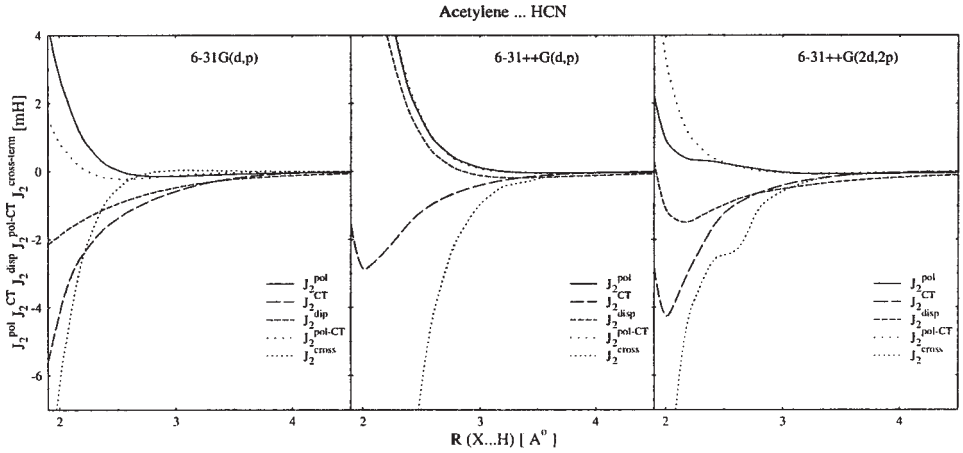

FIGURE 10. Energy components for the Ac . . . HCN system calculated in three different basis sets [6-31G(d,p), 6-31++G(d,p), 6-31++G(2d,2p)] as a function of the r_{HX} hydrogen bond length. The curves display five different components of the J_2 energy: J_2^{pol}, polarization; J_2^{CT}, charge-transfer; J_2^{disp}, dispersion; J_2^{pol-CT}, combined polarization and charge-transfer; J_2^{cross}, second-order "cross" term.

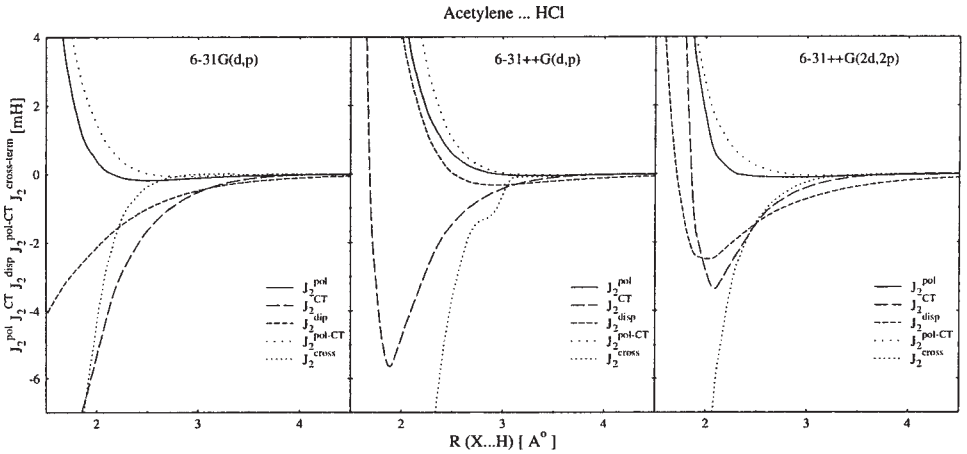

FIGURE 11. Energy components for the Ac . . . HCl system calculated in three different basis sets [6-31G(d,p), 6-31++G(d,p), 6-31++G(2d,2p)] as a function of the r_{HX} hydrogen bond length. The curves display five different components of the J_2 energy: J_2^{pol}, polarization; J_2^{CT}, charge-transfer; J_2^{disp}, dispersion; J_2^{pol-CT}, combined polarization and charge-transfer; J_2^{cross}, second-order "cross" term.

different "physical" energy components near the equilibrium state, it can be ascertained that the CT component provides the dominant contribution. This latter one does not have as strong a basis dependence as it has for the dispersion part. This effect is emphasized more in the case of the Ac . . . HF and the Ac . . . HCl dimers. Dispersion contributions are also significant for all four molecular complexes. Note that these two components have an important influence on the second-order energy J_2. At the same time, the second-order polarization and combined polarization and charge transfer components bring down very fast as the intermolecular distance increases, in order to influence the results. It is also important to know how changes can induce the first-order polarization effects in the results. These contributions could be estimated if we consider the difference between the CHA–MP2 and the CHA–PT2 values. It can be observed from the tables that in the case of the Ac . . . HF and the Ac . . . HCN systems these effects are important, while for the Ac . . . HCl and the Ac . . . AC ones their contributions are smaller.

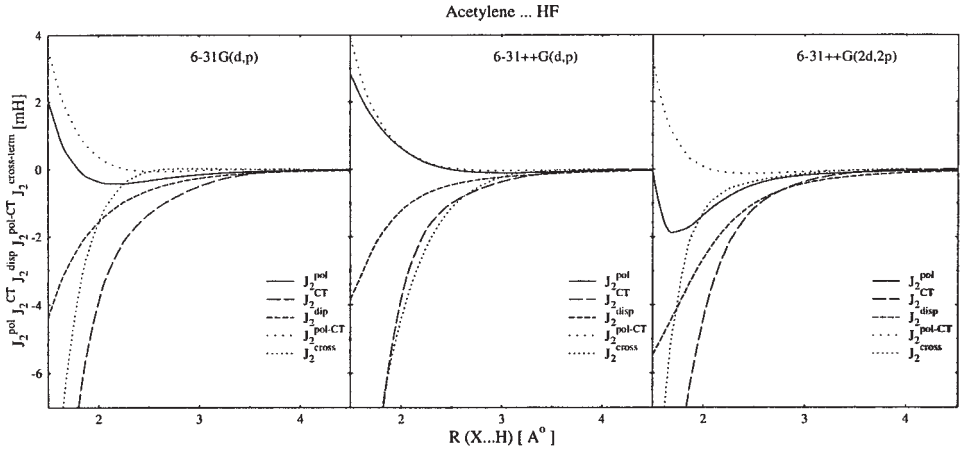

FIGURE 12. Energy components for the Ac . . . HF system calculated in three different basis sets [6-31G(d,p), 6-31++G(d,p), 6-31++G(2d,2p)] as a function of the r_{HX} hydrogen bond length. The curves display five different components of the J_2 energy: J_2^{pol}, polarization; J_2^{CT}, charge-transfer; J_2^{disp}, dispersion; J_2^{pol-CT}, combined polarization and charge-transfer; J_2^{cross}, second-order "cross" term.

5. Conclusions

Considering the results, it can be concluded that the BSSE contents are fairly significant when the perturbation corrections are calculated to study the interactions in weakly bonded molecular systems. The second-order corrections were found to be very large compared to the HF results; this finding stimulates us to perform a detailed study in the field of second-order energy decompositions. It was also obtained that the fourth-order corrections in some cases can yield important contributions in the intermolecular interaction energies (see Acetylene–HCl). This work demonstrates that the experimental results are in good agreement with our BSSE-free values calculated for different intermolecular distances, except for the Ac . . . HF dimer. The second-order energy is dominated by the charge transfer and the dispersion components; however, at a shorter intermolecular distance, the "cross" term would be important.

ACKNOWLEDGMENTS

This work was supported by OTKA grant T037994. G. J. H. acknowledges the Hungarian Academy of Sciences for partially supporting this research through the Grant Bolyai. A. B. thanks the European Union for a fellowship under the contract BMH4-CT96-1618, which funded his study visit to Heidelberg. A. B. is a doctoral student at Foundation for Hungarian Education and Research, Ministry of Education, Hungary, which is gratefully acknowledged.

References

1. Scheiner, S.; Grabowski, S. J. J Mol Struct 2002, 615, 209.
2. Hartmann, M.; Wetmore, S. D.; Radom, L. J Phys Chem 2001, 105, 4470.
3. Vargas, R.; Garza, J.; Friesner, R. A.; Stern, H.; Hay, B. P.; Dixon, D. A. J Phys Chem A 2001, 105, 4963.
4. Rozas, I.; Alkorta, I.; Elguero, J. J Phys Chem 1997, 101, 9457.
5. Alagona, G.; Ghio, C. J. J Mol Struct (Theochem) 1995, 330, 77.
6. Oliveira, G.; Dykstra, C. E. J Mol Struct (Theochem) 1995, 337, 1.
7. Novoa, J. J.; Planas, M.; Rovira, M. C. Chem Phys Lett 1996, 251, 33.
8. Bende, A.; Vibók, Á.; Halász, G. J.; Suhai, S. Int J Quantum Chem 2001, 84, 617.
9. Bende, A.; Knapp-Mohammady, M.; Suhai, S. Int J Quantum Chem 2003, 92(2), 152.
10. Bende, A.; Vibók, Á.; Halász, G. J.; Suhai, S. Int J Quantum Chem 2004, 99, 585.
11. Bende, A.; Vibók, Á.; Halász, G. J.; Suhai, S. Acta Chim Phys Debrecina 2003, XXXVI, 7.
12. Salvador, P.; Simon, S.; Duran, M.; Dannenberg, J. J. J Chem Phys 2000, 113(14), 5666.
13. Salvador, P.; Szczęśniak, M. M. J Chem Phys 2003, 118, 537.
14. Jansen, H. B.; Ross, P. Chem Phys Lett 1969, 3, 140.
15. Boys, S. B.; Bernardi, F. Mol Phys 1970, 19, 553.
16. Mayer, I. Int J Quantum Chem 1983, 23, 341.
17. Mayer, I. Int J Quantum Chem 1998, 70, 41.
18. Mayer, I.; Surján, P. R. Chem Phys Lett 1992, 191, 497.
19. Mayer, I.; Vibók, Á. Chem Phys Lett 1987, 136, 115; Chem Phys Lett 1987, 140, 558.
20. Vibók, Á.; Mayer, I. J Mol Struct (Theochem) 1988, 170, 9.
21. Mayer, I.; Vibók, Á.; Halász, G. J.; Valiron, P. Int J Quantum Chem 1996, 57, 1049; Halász, G. J.; Vibók, Á.; Valiron, P.; Mayer, I. J Phys Chem 1996, 100, 6332.
22. Halász, G. J.; Vibók, Á.; Suhai, S. Int J Quantum Chem 1998, 68, 151.
23. Mayer, I.; Turi, L. J Mol Struct (Theochem) 1991, 227, 43.
24. Mayer, I.; Surján, P. R. Int J Quantum Chem 1989, 36, 225.
25. Mayer, I.; Surján, P. R.; Vibók, Á. Int J Quantum Chem Quant Chem Symp 1989, 23, 281.
26. Mayer, I.; Vibók, Á. Int J Quantum Chem 1991, 40, 139.
27. Vibók, Á.; Mayer, I. Int J Quantum Chem 1992, 43, 801.
28. Hamza, A.; Vibók, Á.; Halász, G. J.; Mayer, I. J Mol Struct (Theochem) 2000, 501, 427.
29. Halász, G. J.; Vibók, Á.; Suhai, S.; Mayer, I. Int J Quantum Chem 2002, 89, 190.
30. Mayer, I.; Vibók, Á. Mol Phys 1997, 92, 503.
31. Vibók, Á.; Halász, G. J.; Mayer, I. Mol Phys 1998, 93, 873.
32. Mayer, I.; Valiron, P. J Chem Phys 1998, 109, 3360.
33. Vibók, Á.; Halász, G. J.; Mayer, I. in Electron Correlation and Material Properties; Gonis, A.; Kioussis, N.; Ciftan, M., Eds.; Kluwer–Academic/Plenum: New York, 2003; p 263–283.
34. Mayer, I.; Valiron, P. Program CHA-MP2, 1998.
35. Valiron, P.; Vibók, Á.; Mayer, I. J Comp Chem 1993, 275, 46.
36. Halász, G. J.; Vibók, Á.; Mayer, I. J Comp Chem 1999, 20, 274.
37. Bende, A.; Vibók, Á.; Halász, G. J.; Suhai, S. Int J Quantum Chem 2001, 84, 617.
38. Mayer, I. Mol Phys 1996, 89, 515.
39. Hamza, A.; Vibók, Á.; Halász, G. J.; Mayer, I. Theor Chem Acc 2001, 107, 38.
40. Frisch, M. J.; Trucks, G. W.; Schlegel, H. B.; Scuseria, G. E.; Robb, M. A.; Cheeseman, J. R.; Zakrzewski, V. G.; Montgomery, J. A.; Stratmann, R. E., Jr.; Burant, J. C.; Dapprich, S.; Millam, J. M.; Daniels, A. D.; Kudin, K. N.; Strain, M. C.; Farkas, O.; Tomasi, J.; Barone, V.; Cossi, M.; Cammi, R.; Mennucci, B.; Pomelli, C.; Adamo, C.; Clifford, S.; Ochterski, J.; Petersson, G. A.; Ayala, P. Y.; Cui, Q.; Morokuma, K.; Malick, D. K.; Rabuck, A. D.; Raghavachari, K.; Foresman, J. B.; Cioslowski, J.; Ortiz, J. V.; Baboul, A. G.; Stefanov, B. B.; Liu, G.; Liashenko, A.; Piskorz, P.; Komaromi, I.; Gomperts, R.; Martin, R. L.; Fox, D. J.; Keith, T.; Al-Laham, M. A.; Peng, C. Y.; Nanayakkara, A.; Gonzalez, C.; Challacombe, M.; Gill, P. M. W.; Johnson, B. W.; Chen, W.; Wong, M. W.; Andres, J. L.; Gonzalez, C.; Head-Gordon, M.; Replogle, E. S.; Pople, J. A. Gaussian: Pittsburgh, PA, 1998.

41. HONDO-8, from MOTECC-91. Contributed and documented by M. Dupuis and A. Farazdel, IBM Corporation Center for Scientific & Engineering Computations: Kingston, NY, 1991.
42. Press, W. H.; Flannery, B. P.; Teukolsky, S. A.; Vetterling, W. T. Numerical Recipes, Cambridge University Press: Cambridge, 1996.
43. Aldrich, P. D.; Kukolich, S. G.; Cambell, E. J. J Chem Phys 1983, 78, 3521.
44. Kukolich, S. G.; Aldrich, P. D.; Read, W. G.; Cambell, E. J. Chem Phys Lett 1982, 90, 329.
45. Legon, A. C.; Aldrich, P. D.; Flygare, W. H. J Chem Phys 1981, 75, 625.
46. Read, W. G.; Flygare, H. J Chem Phys 1982, 76, 2238.